Progress In Electromagnetics Research, Vol. 112, 397–414, 2011

ANALYSIS OF HIGH FREQUENCY PLANE WAVE TRANSMISSION INTO A DOUBLE NEGATIVE CYLINDER BY THE MODIFIED WATSON TRANSFORMATION AND DEBYE SERIES EXPANSION: FIRST TERM OF THE DEBYE SERIES

S. G. Şen

Department of Electrical and Electronics Engineering
Atatürk University, Erzurum 25240, Turkey

Abstract—The modified Watson transform is applied to the Mie series for the electromagnetic wave transmitted into the double negative cylinder due to high frequency plane wave incidence The Debye series expansion is adapted to the transmission coefficients to reveal the transmission mechanism at high frequency. The first term of the Debye series is examined. Two kinds of geometrical shadow regions and two kinds of geometrically lit regions are shown to exist. The field formation mechanisms in these regions are indicated. Several differences between a double positive cylinder and a double negative cylinder are determined The field computations are performed in the geometrical shadow and the geometrically lit regions for the first term of the Debye series. The residue series and steepest descent computations are shown to be in good agreement with the Mie series computations.

1. INTRODUCTION

Double negative (DNG) metamaterials are artificial materials which have negative permittivities and permeabilities. Veselago was the first to propose DNG metamaterials and their basic properties theoretically in the article [1] in 1968. The bases for the physical realizations of DNG metamaterials using split ring resonators and thin wires were set up in [2, 3]. The construction of a DNG metamaterial and the experimental verification of negative refraction were demonstrated in [4, 5]. The L-C loaded transmission line method which is

Received 16 December 2010, Accepted 11 January 2011, Scheduled 25 January 2011
Corresponding author: Saffet Gökçen Şen (gokcen.sen@atauni.edu.tr).

another way of implementing DNG metamaterials was numerically and experimentally exhibited in [6–8]. Some recent work on left-handed metamaterials is cited in [9–15].

The Mie series expansion for the transmitted field due to a high frequency plane wave incident on an infinitely long dielectric cylinder which is a canonical geometry to simulate a smooth convex surface has a computational burden due its slow convergence. In addition, this expansion lacks the physical insight into the transmission process. The modified Watson transform followed by the Debye series expansion eliminates the computational burden and provides the physical insight. The Watson transform was used first in [17] Some other applications of it are given in [18–23]. The Debye series expansion was used first by Debye in [16]. In [24–27], some other applications of the Debye series expansion are given.

In this article, the transmission of a high frequency plane wave into an infinitely long dielectric cylinder is examined for the first term of the Debye series expansion and several differences between a DPS and a DNG cylinder are indicated This article stems from the work done in [28] which was originated from [26, 27, 29]

The article is organized in the following way: In the Section 2, the Mie series expansion of the transmitted field is derived. In the Section 3, the modified Watson transform and the Debye series expansion are applied to the Mie series. In the Section 4, the first term of the Debye series is analyzed. The geometrical shadow regions and the geometrically lit regions are determined. The physical pictures for the field formation in these regions are found out in terms of creeping waves and rays. Using these physical pictures, some comparisons are made between a DPS and a DNG cylinder. In the Section 5, the numerical results are presented to verify the physical pictures derived in the Section 4.

2. THE MIE SERIES EXPANSION FOR THE TRANSMITTED FIELD

Assuming a time harmonic dependence of $e^{-j\omega t}$, the dielectric cylinder of infinite length and of radius a is illuminated by an incident plane of the form

$$\vec{E}^i = \hat{a}_z e^{-jk_0 x} \tag{1}$$

with

$$k_0 = \omega\sqrt{\mu_0 \varepsilon_0} \tag{2}$$

ω is the radial frequency of the incident plane wave. ε_0 is the permittivity of the free space and μ_0 is the permeability of the free space.

The problem geometry is shown in Figure 1.

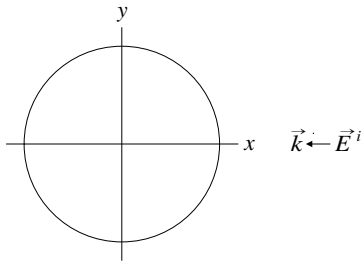

Figure 1. The problem geometry.

The Mie series expansions of the incident and transmitted fields are

$$\vec{E}^i = \hat{a}_z \sum_{l=-\infty}^{\infty} j^{-l} J_l\left(k_0\rho\right) e^{jl\phi} \tag{3}$$

$$\vec{E}^t = \hat{a}_z \sum_{l=-\infty}^{\infty} d_l \; J_l\left(nk_0\rho\right) e^{jl\phi} \tag{4}$$

where $j = \sqrt{-1}$, (ρ, ϕ) is the cylindrical coordinate pair of the field point and d_l are the Mie series coefficients of the transmitted field.

Applying the boundary conditions at the boundary of the cylinder of the refractive index n, the transmission coefficients are found to be

$$d_l = j^{-l} \frac{\left[J_l\left(\beta\right) H_l^{(1)'}\left(\beta\right) - J_l'\left(\beta\right) H_l^{(1)}\left(\beta\right)\right]}{\left[J_l\left(\alpha\right) H_l^{(1)'}\left(\beta\right) - \frac{n}{\mu_r} J_l'\left(\alpha\right) H_l^{(1)}\left(\beta\right)\right]} \tag{5}$$

where

$$\beta = k_o a \quad \alpha = n\beta \tag{6}$$

The definition for $f'\left(z_0\right)$ where $f\left(z_0\right)$ is either $J_l\left(\beta\right)$ or $H_l^{(1)}\left(\beta\right)$ in (5) is given as follows:

$$f'\left(z_0\right) = \left.\frac{\partial f}{\partial z}\right|_{z=z_0}. \tag{7}$$

3. THE MODIFIED WATSON TRANSFORM AND THE DEBYE SERIES EXPANSION

In order to overcome the computational burden of the Mie series solution, the Modified Watson transform is applied to the Mie series

solution. Before the application of the modified Watson transform, the Bessel function of the first kind is separated into its Hankel function components. This separation is made for the field points outside the circle which has a radius $\frac{a}{|n|}$ and has its center at the origin since a physical interpretation appropriate for this field region is to be made. The application of the modified Watson transform to the Mie series expression yields the following equality:

$$E^d = \sum_{l=-\infty}^{\infty} d_l J_l\left(nk_0\rho\right) e^{jl\phi} = -\frac{1}{2j} \int_{-\infty+j\varepsilon}^{\infty+j\varepsilon}$$
$$\left[0.5d_{-v}H_{-v}^{(1)}\left(nk_0\rho\right) e^{jv(\phi-\pi)} + 0.5d_v H_v^{(1)}\left(nk_0\rho\right) e^{-jv(\phi-\pi)}\right]$$
$$\left[2\sum_{m=0}^{\infty}(-1)^m e^{j(2m+1)\pi\left(v-\frac{1}{2}\right)}\right] dv$$
$$-\frac{1}{2j} \int_{-\infty+j\varepsilon}^{\infty+j\varepsilon} \left[0.5d_{-v}H_{-v}^{(2)}\left(nk_0\rho\right) e^{jv(\phi-\pi)} + 0.5d_v H_v^{(2)}\left(nk_0\rho\right) e^{-jv(\phi-\pi)}\right]$$
$$\left[2\sum_{m=0}^{\infty}(-1)^m e^{j(2m+1)\pi\left(v-\frac{1}{2}\right)}\right] dv \tag{8}$$

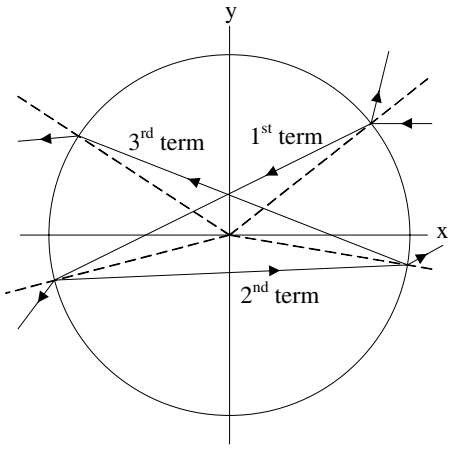

Figure 2. The physical picture for the high frequency transmission problem.

At sufficiently high frequencies of operation, the incident plane wave can be considered to be made up of rays incident on the dielectric cylinder. Then, the physical picture shown in Figure 2 can be used for the transmission problem. The ray incident on the cylinder is transmitted into the cylinder. This transmitted ray is the first term contributing to the field inside the cylinder. The first term ray is reflected by the cylinder to form the second term. This second term ray is reflected by the cylinder to form the third term. Continuing in this manner, the pth term contributing to the field inside the cylinder is obtained after $p-1$ reflections inside the cylinder. The ray incident on the cylinder is made up of cylindrical waves. Hence, a transmission coefficient and a reflection coefficient will be in charge for the cylindrical waves during the field formation inside the cylinder. R_{11} is the reflection coefficient for the cylindrical wave reflected from the 1st medium, the interior of the cylinder, to the 1st medium. T_{21} is the transmission coefficient for cylindrical wave transmitted from the 2nd medium, the exterior of the cylinder, to the 1st medium.

The mathematical expressions for R_{11} and T_{21} are

$$R_{11} = -\frac{[1\ \beta] - \frac{n}{\mu_r}[1\ \alpha]}{[1\ \beta] - \frac{n}{\mu_r}[2\ \alpha]} \quad T_{21} = \frac{4j}{\pi\beta H_v^{(1)}(\beta) H_v^{(2)}(\beta)\left([1\ \beta] - \frac{n}{\mu_r}[2\ \alpha]\right)} \tag{9}$$

where

$$[1\ x] \triangleq \frac{H_v^{(1)'}(x)}{H_v^{(1)}(x)} \quad [2\ x] \triangleq \frac{H_v^{(2)'}(x)}{H_v^{(2)}(x)} \tag{10}$$

as established in [26]. The transmission and then multiple reflections of the component cylindrical functions can be expressed as a series. The incident cylindrical wave denoted by $H_l^{(2)}(k_0\rho)$ is multiplied by T_{21} and scaled by $H_l^{(2)}(\alpha)$ at the boundary $\rho = a$ to obtain the amplitude of the transmitted cylindrical wave which is the first term of the series. After travelling inside the cylinder, the cylindrical wave hits the cylinder from the interior as a Hankel function of the first kind. It is multiplied by R_{11} and scaled by $H_l^{(2)}(\alpha)$ to obtain the amplitude of the reflected cylindrical wave which is the second term of the series. The series terms are formed in this manner and the following equation is obtained for this series:

$$H_l^{(2)}(\beta)\, T_{21} \frac{1}{H_l^{(2)}(\alpha)} \left[1 + R_{11}\frac{H_l^{(1)}(\alpha)}{H_l^{(2)}(\alpha)} + R_{11}\frac{H_l^{(1)}(\alpha)}{H_l^{(2)}(\alpha)} R_{11}\frac{H_l^{(1)}(\alpha)}{H_l^{(2)}(\alpha)} + \ldots\right]$$

$$= H_l^{(2)}(\beta)\, T_{21} \frac{1}{H_l^{(2)}(\alpha)} \sum_{p=1}^{\infty} \left[R_{11}\frac{H_l^{(1)}(\alpha)}{H_l^{(2)}(\alpha)}\right]^{p-1}. \tag{11}$$

If the condition

$$\left| R_{11} \frac{H_l^{(1)}(\alpha)}{H_l^{(2)}(\alpha)} \right| < 1 \tag{12}$$

is satisfied, then

$$d_l = j^{-l} H_l^{(2)}(\beta)\, T_{21} \frac{1}{H_l^{(2)}(\alpha)} \sum_{p=1}^{\infty} \left[R_{11} \frac{H_l^{(1)}(\alpha)}{H_l^{(2)}(\alpha)} \right]^{p-1} \tag{13}$$

Hence, the series obtained using the physical interpretation converges to the transmission coefficient and the Debye expansion has been applied to the transmission coefficients.

4. THE FIRST TERM OF THE DEBYE SERIES EXPANSION

The application of the Debye expansion to the transmission coefficient has yielded the equation in (13). The transmitted field due to the first term of the Debye expansion is obtained by setting p to 1 in (13) and putting the resulting expression in place of d_v and d_{-v} in (8). In addition, m is set to 0 to obtain the following:

$$E_{t_{p=1}}\big|_{m=0} = \int_{-\infty+j\varepsilon}^{\infty+j\varepsilon} \left\{ 0.5 T_{21} \frac{H_v^{(2)}(\beta)}{H_v^{(2)}(\alpha)} H_v^{(1)}(nk_0\rho) \left[e^{jv\left(\phi+\frac{3\pi}{2}\right)} + e^{-jv\left(\phi-\frac{3\pi}{2}\right)} \right] \right\} dv + \int_{-\infty+j\varepsilon}^{\infty+j\varepsilon} \left\{ 0.5 T_{21} \frac{H_v^{(2)}(\beta) T_{21}(v,\beta)}{H_v^{(2)}(\alpha)} H_v^{(2)}(nk_0\rho) \left[e^{jv\left(\phi-\frac{\pi}{2}\right)} + e^{-jv\left(\phi-\frac{3\pi}{2}\right)} \right] \right\} dv \tag{14}$$

The first integral containing $H_v^{(1)}(nk_0\rho)$ denotes the field formation due to the second intersection of a ray with the field circle. The field circle is the ρ one whose radius is the coordinate of the field point and whose center is the center of the cylinder. The second integral containing $H_v^{(2)}(nk_0\rho)$ denotes the field formation due to the first intersection of the same ray with the field circle. The Figure 3 displays these intersections.

The loci of the points of the first intersection of the ray with the field circle cannot cover the whole field circle. The same case is valid for the loci of the points of the second intersection of the ray with the field circle. Hence, there are two geometrical shadow regions and two geometrically lit regions. In Figure 4 for a DPS cylinder, it is shown that the geometrically lit region for the first intersection is the blue arc

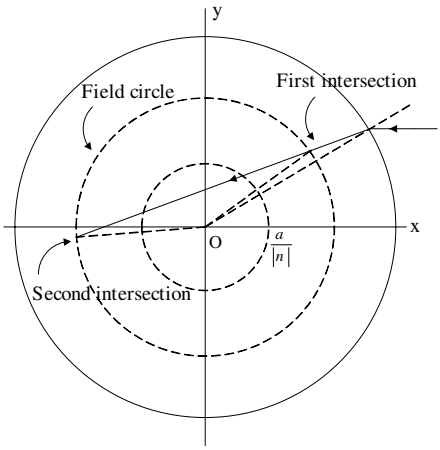

Figure 3. The intersections of a ray with the field circle (DPS).

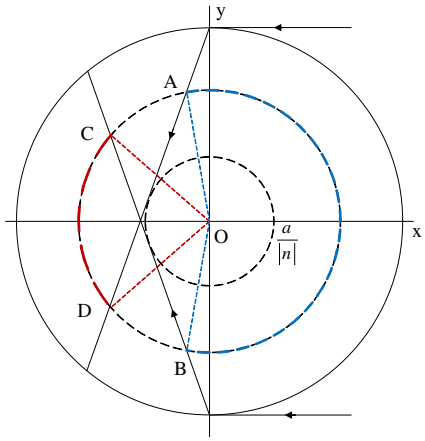

Figure 4. The geometrically lit regions of the first and the second intersections of the first term of the Debye series (DPS).

and the geometrically lit region for the second intersection is the red arc $\widehat{CD}$. Both of the arcs $\widehat{AB}$ are on the field circle. The geometrically lit region for the first term of the transmitted field is the union of these two geometrically lit regions and the geometrical shadow region for the first term of the transmitted field is the intersection of these two geometrical shadow regions.

For a DNG cylinder, in the appropriate field region, the first integral in (14) satisfies

$$\int_{-\infty+j\varepsilon}^{\infty+j\varepsilon} \left\{ 0.5T_{21} \frac{H_v^{(2)}(\beta)}{H_v^{(2)}(\alpha)} H_v^{(1)}(nk_0\rho) \left[e^{jv\left(\phi+\frac{3\pi}{2}\right)} + e^{-jv\left(\phi-\frac{3\pi}{2}\right)} \right] \right\} dv$$

$$= 2\pi j \sum_k \left[\frac{\left(2j \frac{H_{v_k}^{(2)}(|nk_0\rho|)\left[e^{jv_k\left(\phi-\frac{\pi}{2}\right)} + e^{-jv_k\left(\phi+\frac{\pi}{2}\right)} \right]}{\pi\beta H_{v_k}^{(1)}(\beta) H_{v_k}^{(1)}(|\alpha|)} \right)}{\left(\frac{d}{dv} \left([1\ \beta] + \frac{n}{\mu_r} [1\ \ |\alpha|] \right) \right)\Big|_{v=v_k}} \right] \tag{15}$$

If the Debye asymptotic expansion is used for $H_{v_k}^{(2)}(|nk_0\rho|)$ in the residue series, then the following exponential part is obtained for a

prospective physical interpretation:

$$\exp\left\{j\left[-\left(|nk_0\rho|^2-v_k^2\right)^{\frac{1}{2}}-\left(|\alpha|^2-v_k^2\right)^{\frac{1}{2}}-\left(\beta^2-v_k^2\right)^{\frac{1}{2}}+v_k\cos^{-1}\left(\frac{v_k}{|nk_0\rho|}\right)\right.\right.$$
$$\left.\left.+v_k\cos^{-1}\left(\frac{v_k}{|\alpha|}\right)+v_k\cos^{-1}\left(\frac{v_k}{\beta}\right)\right]\right\}\left[e^{jv_k\left(\phi-\frac{\pi}{2}\right)}+e^{-jv_k\left(\phi+\frac{\pi}{2}\right)}\right] \quad (16)$$

Approximating v_k with β, the following simpler form of the first part of the expression in (16) is obtained:

$$\exp\left\{j\,|nk_0|\left[-\left(\rho^2-\left(\frac{a}{|n|}\right)^2\right)^{\frac{1}{2}}-\left(a^2-\left(\frac{a}{|n|}\right)^2\right)^{\frac{1}{2}}\right]\right\}$$
$$\exp\left\{jk_0a\left[\cos^{-1}\left(\frac{\frac{a}{|n|}}{\rho}\right)+\cos^{-1}\left(\frac{1}{|n|}\right)+\left(\phi-\frac{\pi}{2}\right)\right]\right\} \quad (17)$$

From Figure 5, the following geometrical relations can be derived:

$$|T_1T_2|=\left[a^2-\left(\frac{a}{|n|}\right)^2\right]^{\frac{1}{2}} \qquad |T_2F|=\left[\rho^2-\left(\frac{a}{|n|}\right)^2\right]^{\frac{1}{2}}$$
$$\widehat{POT_1}=\phi-\frac{\pi}{2}+\cos^{-1}\left(\frac{\frac{a}{|n|}}{\rho}\right)+\cos^{-1}\left(\frac{1}{|n|}\right) \quad (18)$$

The ray incident on the point P in Figure 5 has the exponential dependence $e^{-jk_0\cos\left(\frac{\pi}{2}\right)}$. It creeps over the cylinder to the point T_1 to have the exponential dependence of $\exp\left(jk_0a\widehat{POT_1}\right)$. Then, it is critically and negatively refracted into the DNG cylinder. It propagates to the field point $F(\rho,\phi)$ with a final exponential dependence of $\exp\left(jk_0a\widehat{POT_1}\right)\exp\left[-j\,|nk_0|\left(|T_1T_2|+|T_2F|\right)\right]$ which is the same as the expression in (17). The negative sign is due to the fact that in a DNG medium, the phase velocity direction is opposite to the direction of the power propagation. The physical interpretation in terms of the phase for the first part of the residue series in (15) is given with this explanation using the geometrical optics (GO). The verification of this physical picture in terms of the amplitude will numerically be made. A similar explanation for the second part of the residue series can be constructed using the ray which is incident on the point Q in Figure 5 and is responsible for the field formation at the field point $F(\rho,-\phi)$.

A similar physical interpretation can be derived for the residue series form of the first part of the second integral in (14). This physical picture is shown in Figure 6.

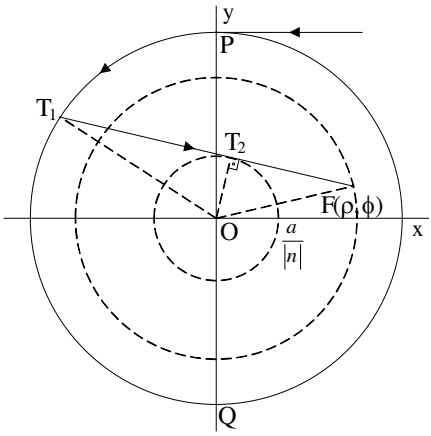

Figure 5. The physical interpretation for the field formation in the geometrical shadow of the second intersection for a double negative cylinder for the first term of the Debye series.

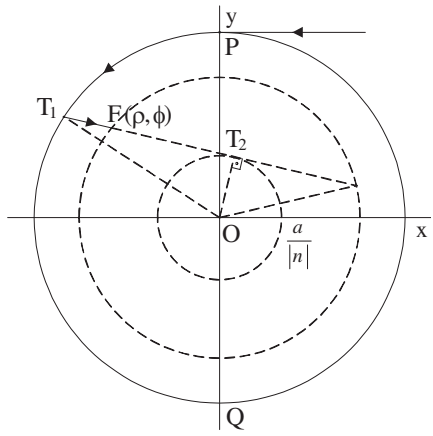

Figure 6. The physical interpretation for the field formation in the geometrical shadow of the first intersection for a double negative cylinder for the first term of the Debye series.

After the examination of the geometrical shadow regions, it is time to consider the geometrically lit regions. The fields in the geometrically lit regions are formed partially by the refracted rays and partially by the refracted creeping waves. The field integrals will be calculated using the steepest descent method (SDM) to calculate the contribution by the refracted rays.

For a DNG cylinder, the following steepest descent equation can be obtained from the first part of the second integral in (14):

$$j\left[-\cos^{-1}\left(\frac{v}{|nk_0\rho|}\right)+\cos^{-1}\left(\frac{v}{|\alpha|}\right)+\cos^{-1}\left(\frac{v}{\beta}\right)+\left(\phi-\frac{\pi}{2}\right)\right]=0 \quad (19)$$

From Figure 7, the following geometrical relations can be written:

$$\cos^{-1}\left(\frac{\frac{a}{|n|}\sin\theta}{a}\right) = \cos^{-1}\left(\frac{\frac{a}{|n|}\sin\theta}{\rho}\right) + \theta - \phi \quad (20)$$

$$|PF| = \left[a^2-\left(\frac{a}{|n|}\sin\theta\right)^2\right]^{\frac{1}{2}} - \left[\rho^2-\left(\frac{a}{|n|}\sin\theta\right)^2\right]^{\frac{1}{2}} \quad (21)$$

If the saddle point solution

$$v=\beta\sin\theta \quad (22)$$

is used in the steepest descent equation, then the geometrical relation in (20) is reached. If the Debye asymptotic expansion is applied to the integrand of the first part of the second integral in (14) and the resulting exponential part is evaluated at the saddle point, then

$$\exp\left\{-j\,|nk_0|\left[-\left(\rho^2-\left(\frac{a}{|n|}\sin\theta\right)^2\right)^{\frac{1}{2}}+\left(a^2-\left(\frac{a}{|n|}\sin\theta\right)^2\right)^{\frac{1}{2}}\right]\right\}$$
$$\exp\left[-jk_0a\cos\left(\theta\right)\right] \tag{23}$$

is obtained. The ray incident on the point P in Figure 7 is denoted mathematically by $\exp\left[-jk_0a\sin\left(\theta\right)\right]$. After being negatively refracted into the cylinder, the ray propagates to the field point with a final exponential dependence of $\exp\left[-jk_0a\cos\left(\theta\right)\right]\exp\left[-j\,|nk_0|\,|PF|\right]$. This final dependence is perceived to be the same as the expression in (23) if the relation in (21) is noticed. Hence, the physical picture shown in Figure 7 is verified in terms of the phase using GO. The verification in terms of the amplitude will numerically be made. A parallel interpretation can be employed for the field formation at the point $F\left(\rho,-\phi\right)$ using the ray incident on the point $P\left(\rho,-\theta\right)$.

A similar physical interpretation can be derived for first part of the first integral in (14). This physical picture for a DNG cylinder is shown in Figure 8.

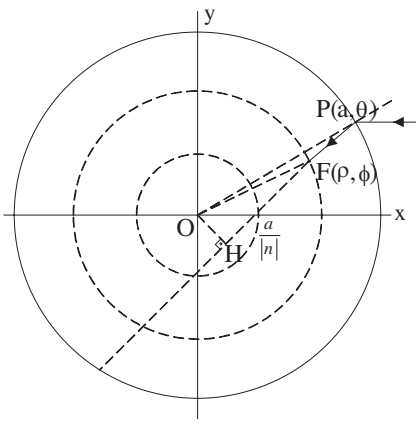

Figure 7. The physical picture for the field formation in the geometrically lit region of the first intersection for a double negative cylinder for the first term of the Debye series.

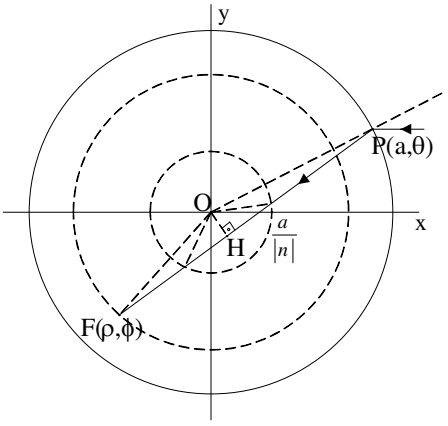

Figure 8. The physical picture for the field formation in the geometrically lit region of the second intersection for a double negative cylinder for the first term of the Debye series.

After exhibiting the field formation mechanisms of the creeping waves and the rays, some differences between a DPS cylinder and a DNG cylinder will be pointed out.

The regions which are not illuminated by the transmitted rays belong to the geometrical shadow region of the related intersection. Then, it can be deduced that DNG cylinders have no geometrical shadow regions for the first term of the Debye series. An implication of the fact that DNG cylinders have no geometrical shadow regions is that two creeping waves can never be in charge for the formation of the transmitted field due to the first term of the Debye series in a DNG cylinder.

On the other hand, DPS cylinders always have geometrical shadow regions The geometrically lit region of the first intersection and the geometrically lit region of the second intersection can never intersect with each other in a DPS cylinder. Hence, due to such an intersection, two rays can never be in charge for the formation of the transmitted field in a DPS cylinder for the first term of the Debye series.

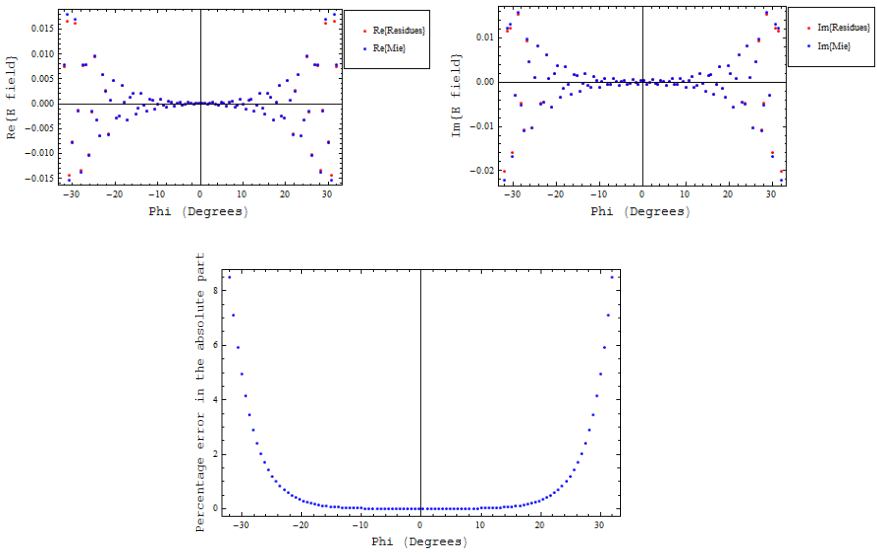

Figure 9. The geometrical shadow region of the second intersection, $n = -3$, $\beta = 50\pi$, $\rho = (29/38)a$.

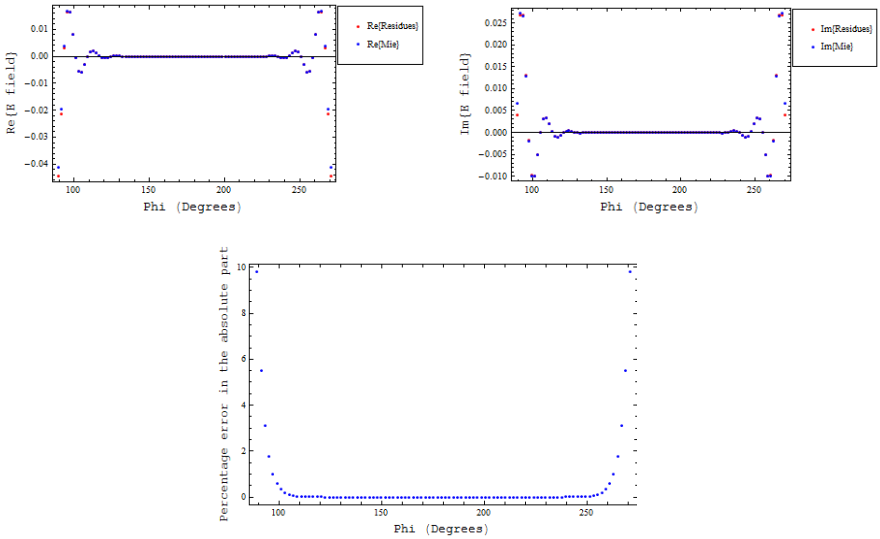

Figure 10. The geometrical shadow region of the first intersection, $n = -3$, $\beta = 50\pi$, $\rho = (29/38)a$.

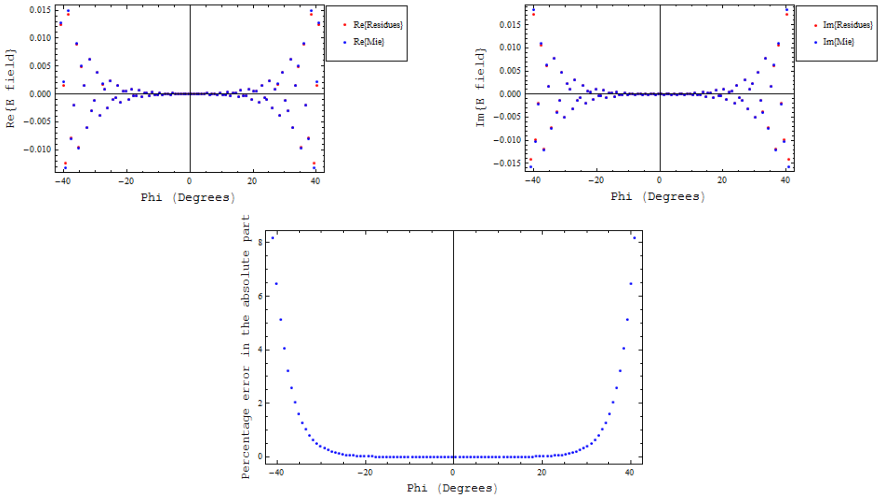

Figure 11. The geometrical shadow region of the second intersection, $n = -3.50$, $\beta = 50\pi$, $\rho = (61/76)a$.

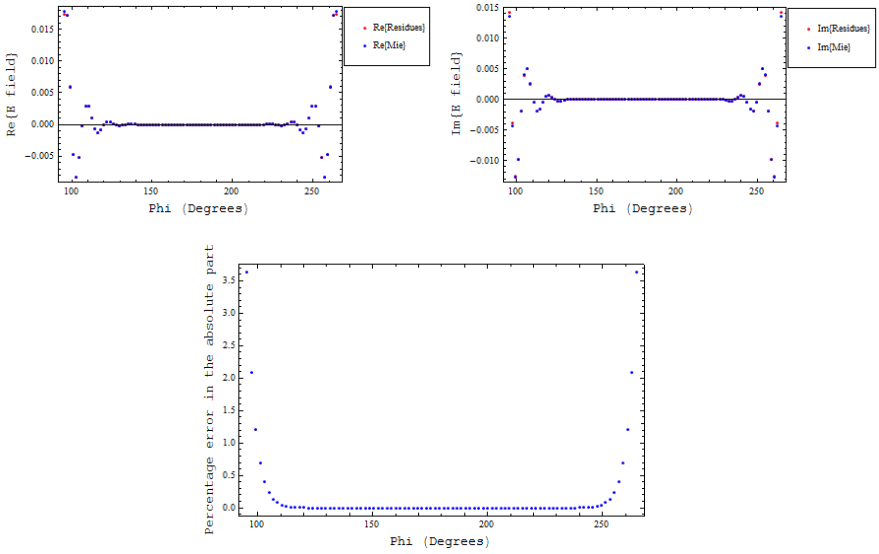

Figure 12. The geometrical shadow region of the first intersection, $n = -3.50$, $\beta = 50\pi$, $\rho = (61/76)a$.

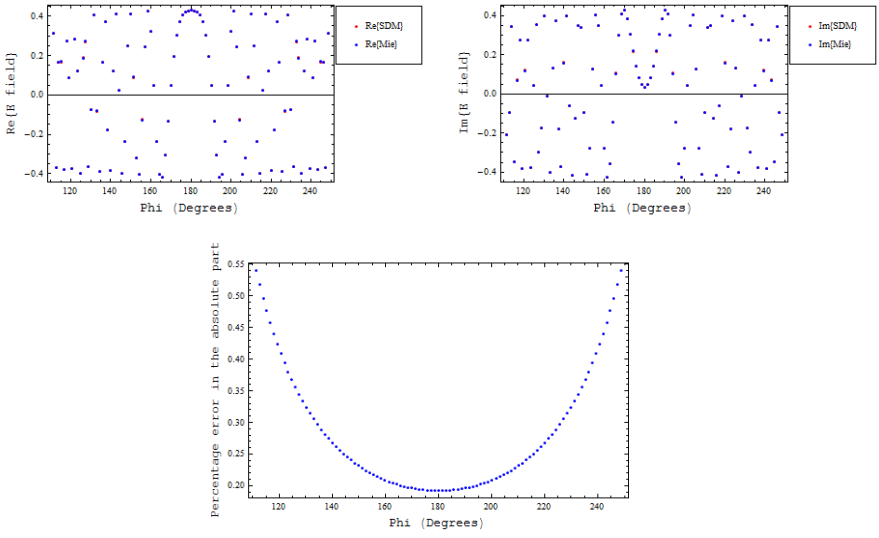

Figure 13. The geometrically lit region of the second intersection, $n = -3$, $\beta = 50\pi$, $\rho = (29/38)a$.

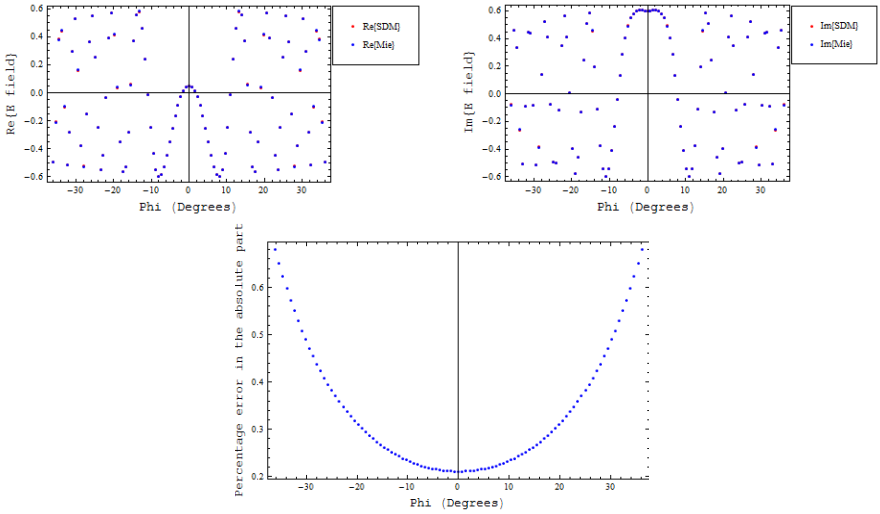

Figure 14. The geometrically lit region of the first intersection, $n = -3$, $\beta = 50\pi$, $\rho = (29/38)a$.

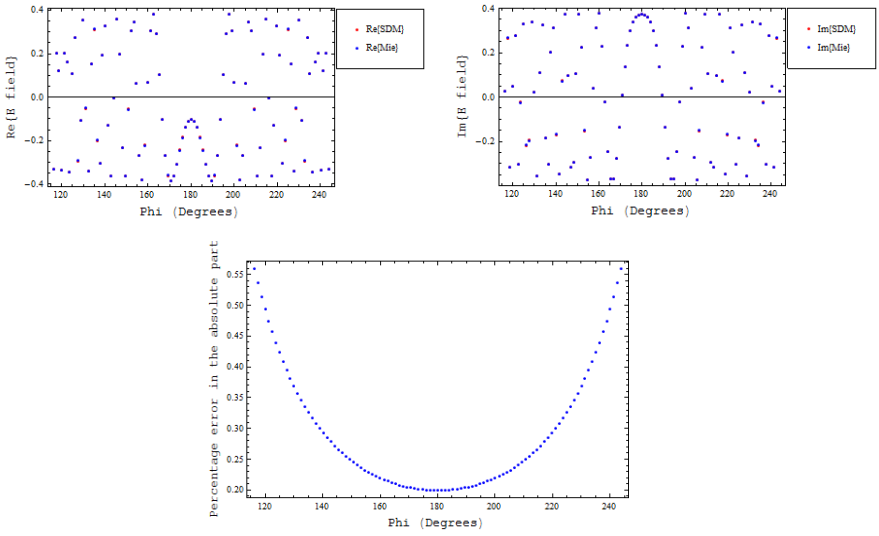

Figure 15. The geometrically lit region of the second intersection, $n = -3.50$, $\beta = 50\pi$, $\rho = (61/76)a$.

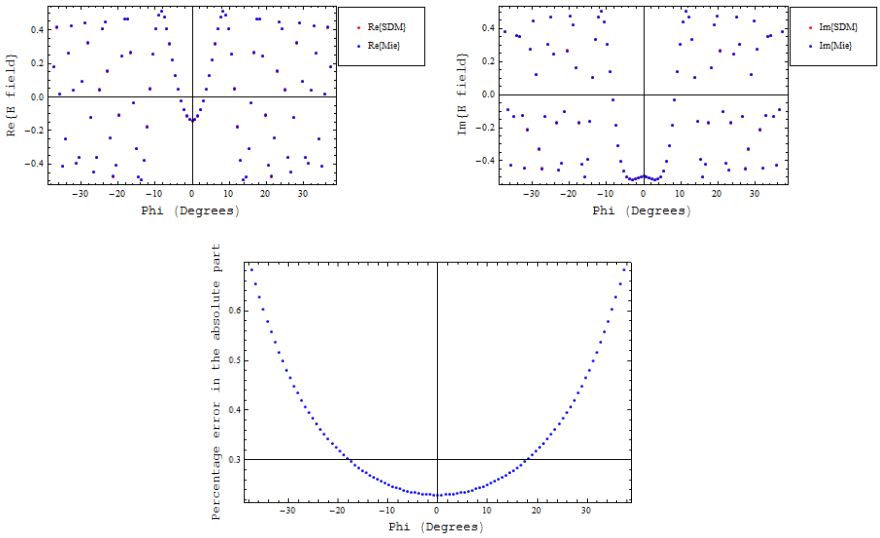

Figure 16. The geometrically lit region of the first intersection, $n = -3.50$, $\beta = 50\pi$, $\rho = (61/76)a$.

5. NUMERICAL RESULTS

The field computations are made for the geometrical shadow regions and the geometrically lit regions of the first and second intersections. The percentage error in a result is defined as follows:

$$percentage\ error = 100 \times \frac{|(Mie\ series\ result) - (residue\ series\ result\ or\ SDM\ result)|}{|Mie\ series\ result|} \quad (24)$$

From the calculation results given in Figures 9–16, it can be seen that the agreement between the Mie series results and the residue series results and the agreement between the Mie series results and the SDM results are very good. This agreement is uniform throughout the field points. Hence, the physical pictures and the related results presented in the previous section are proven to be true.

In addition to the verification of the physical pictures derived in the previous section, the computations reveal the speed advantage of the residue series method and the SDM. The residue series method is approximately 60 times faster than the Mie series method, and the SDM is approximately 220 times faster than the Mie series method.

6. CONCLUSION

The modified Watson transform and the Debye series expansion have been adapted to the transmission of a high frequency plane wave into an infinitely long DNG cylinder. The first term of the Debye series has been examined. The existence of two kinds of geometrical shadow regions and two kinds of geometrically lit regions has been observed. The field formation mechanisms and the related physical pictures have been determined. The phase verification of the physical pictures has been made using the geometrical optics and the amplitude verification has been made by numerical simulation. The numerical simulation results have been observed to be very accurate. Hence, the modified Watson transform and the Debye series expansion reveals the physical picture of the transmission. DNG and DPS cylinders have been compared in terms of the existence of the geometrical shadow region and field formation mechanisms Negative refraction and the backward wave propagation in a DNG medium have been verified.

REFERENCES

1. Veselago, V. G., "The electrodynamics of substances with simultaneously negative values of ε and μ," *Soviet Physics Uspekhi*, Vol. 10, No. 4, Jan.–Feb. 1968.
2. Pendry, J. B., A. J. Holden, D. J. Robbins, and W. J. Stewart, "Magnetism from conductors and enhanced nonlinear phenomena," *IEEE Transactions on Microwave Theory and Techniques*, Vol. 47, 2075–2084, Nov. 1999.
3. Pendry, J. B., A. J. Holden, W. J. Stewart, and I. Youngs, "Extremely low frequency plasmons in metallic mesostructures," *Physical Review Letters*, Vol. 76, 4773, Jun. 17, 1996.
4. Smith, D. R., W. J. Padilla, D. C. Vier, S. C. Nemat-Nasser, and S. Schultz, "Composite medium with simultaneously negative permeability and permittivity," *Physical Review Letters*, Vol. 84, 4184, May 1, 2000.
5. Shelby, R. A., D. R. Smith, and S. Schultz, "Experimental verification of a negative index of refraction," *Science*, Vol. 292, Apr. 6, 2001.
6. Caloz, C., H. Okabe, T. Iwai, and T. Itoh, "Transmission line approach of left-handed (LH) materials," *Proc. USNC/URSI National Radio Science Meeting*, Vol. 1, 39, San Antonio, TX, Jun. 2002.
7. Iyer, A. K. and G. V. Eleftheriades, "Negative refractive index

metamaterials supporting 2-D waves," *Proc. IEEE MTT-S Int. Symp.*, Vol. 2, 1067–1070, San Antonio, TX, Jun. 2002.

8. Eleftheriades, G. V., A. K. Iyer, and P. C. Kramer, "Planar negative refractive index media using periodically L-C loaded transmission lines," *IEEE Transactions on Microwave Theory and Techniques*, Vol. 50, No. 12, Dec. 2002.
9. Naghsvarian-Jahromi, M., "Novel compact meta-material tunable quasi elliptic band-pass filter using microstrip to slotline transition," *Journal of Electromagnetic Waves and Applications*, Vol. 24, No. 17–18, 2371–2382, 2010.
10. Choi, J. and S. Lim, "Frequency and radiation pattern reconfigurable small metamaterial antenna using its extraordinary zeroth-order resonance," *Journal of Electromagnetic Waves and Applications*, Vol. 24, No. 14–15, 2119–2127, 2010.
11. Alici, K. B., A. E. Serebryannikov, and E. Ozbay, "Radiation properties and coupling analysis of a metamaterial based, dual polarization, dual band, multiple split ring resonator antenna," *Journal of Electromagnetic Waves and Applications*, Vol. 24, No. 8–9, 1183–1193, 2010.
12. Sabah, C., "Tunable metamaterial design composed of triangular split ring resonator and wire strip for S- and C-microwave bands," *Progress In Electromagnetics Research B*, Vol. 22, 341–357, 2010.
13. Wang, J., S. Qu, H. Ma, J. Hu, Y. Yang, X. Wu, Z. Xu, and M. Hao, "A dielectric resonator-based route to left-handed metamaterials," *Progress In Electromagnetics Research B*, Vol. 13, 133–150, 2009.
14. Penalosa-Camacho, C., T. M. Martin-Guerrero, J. Esteban, and J. E. Page, "Derivation and general properties of artificial lossless balanced composite right/left-handed transmission lines of arbitrary order," *Progress In Electromagnetics Research B*, Vol. 13, 151–169, 2009.
15. Qiang, L., H. Lu, W. Zhao, J.-K. Wang, and B. Liu, "Simplified extended composite right/left-handed transmission line structure for dual-band applications," *Progress In Electromagnetics Research Letters*, Vol. 15, 137–144, 2010.
16. Debye, P., "Das elektromagnetische feld um ein zylinder und die theorie des regenbogens," *Physik. Z.*, Vol. 9, 775, 1908.
17. Watson, G. N., "The diffraction of electric waves by the earth," *Proceedings of the Royal Society of London*, Vol. 95, No. 666, 83–99, 1918.
18. Pumplin, J., "Application of Sommerfeld-Watson transformation

to an electrostatics problem," *American Journal of Physics*, Vol. 37, No. 7, 737–739, 1969.

19. Uberall, H., "Acoustic scattering from elastic cylinders and spheres: Surface waves (Watson transform) and transmitted waves," *Diffusion et Diffraction*, Vol. 2, No. 5, 353–387, 1985.
20. Li, M. K. and W. C. Chew, "A new Sommerfeld-Watson transformation in 3-D," *IEEE Antennas and Wireless Propagation Letters*, Vol. 3, 75–78, Dec. 2004.
21. Wang, H.-L., Q. Wu, X.-J. He, J. Wu, and L.-W. Li, "Computation of wave scattering problems from a spheric body: Derivation of the new Sommerfeld-Watson transformation," *PIERS Online*, Vol. 1, No. 6, 707–710, 2005.
22. Valagiannopoulos, C. A., "An overview of the Watson transformation presented through a simple example," *Progress In Electromagnetics Research*, Vol. 75, 137–152, 2007.
23. Sha, W. E. I. and W. C. Chew, "High frequency scattering from an impenetrable sphere," *Progress In Electromagnetics Research*, Vol. 97, 291–325, 2009.
24. Inada, H., "Diffracted field computations by a series expansion," *Radio Science*, Vol. 10, 205–220, Feb. 1975.
25. Sasamori, T., T. Uno, and S. Adachi, "High-frequency analysis of electromagnetic scattering due to a dielectric cylinder," *Electronics and Communications in Japan Part II — Electronics*, Vol. 78, No. 4, 41–55, 1995.
26. Nussenzweig, H. M., "High-frequency scattering by a transparent sphere. 1. Direct reflection and transmission," *Journal of Mathematical Physics*, Vol. 10, No. 1, 82–124, Jan. 1969.
27. Nussenzweig, H. M., "High-frequency scattering by an impenetrable sphere," *Annals of Physics*, Vol. 34, 23–95, 1965.
28. Şen, S. G. and M. Kuzuoğlu, "Analysis of high frequency plane wave scattering from a double negative cylinder via the Modified Watson transformation and Debye expansion," *Progress In Electromagnetics Research*, Vol. 84, 55–92, 2008.
29. Şen, S. G., *Investigation of Electromagnetic Wave Propagation in Double Negative Metamaterials*, Ph.D. Thesis, Middle East Technical University, Ankara, Türkiye, 2008, http://etd.lib.metu.edu.tr/upload/12609748/index.pdf.